Biochimica et Biophysica Acta 1818 (2012) 154–161

Contents lists available at SciVerse ScienceDirect

Biochimica et Biophysica Acta

journal homepage: www.elsevier.com/locate/bbamem

Förster resonance energy transfer as a probe of membrane protein folding ☆

Guipeun Kang, Ignacio López-Peña, Vanessa Oklejas, Cyril S. Gary, Weihan Cao, Judy E. Kim *

Department of Chemistry and Biochemistry, University of California at San Diego, La Jolla, CA 92093, USA

ARTICLE INFO

Article history:
Received 26 June 2011
Received in revised form 24 August 2011
Accepted 25 August 2011
Available online 7 September 2011

Keywords:
Fluorescence
Tryptophan
OmpA
IAEDANS
Vesicle
Bilayer

ABSTRACT

The folding reaction of a β-barrel membrane protein, outer membrane protein A (OmpA), is probed with Förster resonance energy transfer (FRET) experiments. Four mutants of OmpA were generated in which the donor fluorophore, tryptophan, and acceptor molecule, a naphthalene derivative, are placed in various locations on the protein to report the evolution of distances across the bilayer and across the protein pore during a folding event. Analysis of the FRET efficiencies reveals three timescales for tertiary structure changes associated with insertion and folding into a synthetic bilayer. A narrow pore forms during the initial stage of insertion, followed by bilayer traversal. Finally, a long-time component is attributed to equilibration and relaxation, and may involve global changes such as pore expansion and strand extension. These results augment the existing models that describe concerted insertion and folding events, and highlight the ability of FRET to provide insight into the complex mechanisms of membrane protein folding. This article is part of a Special Issue entitled: Membrane protein structure and function.

1. Introduction

In the energy landscape theory of protein folding [1–3], favorable contacts bias a nascent protein toward a three-dimensional structure that represents the global free energy minimum. The non-covalent intramolecular forces that contribute to the stability of the native structure have been characterized for soluble proteins [4]. In the case of membrane proteins, additional intermolecular interactions between the protein and lipid bilayer must be considered, but are not well understood.

Knowledge of the chemical and physical properties of the bilayer is essential for understanding membrane protein structure and folding. A bilayer exhibits at least two distinct chemical regions, the interfacial space and the hydrophobic core [5]. The interfacial region, which spans ~15 Å, is chemically heterogeneous and contains functional groups that may participate in hydrogen bonds and ionic interactions [6]. This region is important for backbone solvation and can induce secondary structure in a peptide that is otherwise unfolded in aqueous solution [7,8]. In the hydrophobic core, the low dielectric constant of ~2 may enhance some molecular interactions [9,10]. For example, the energies of backbone hydrogen bonds in water and in the bilayer have been calculated to be ~1 kcal/mol and ~5 kcal/mol, respectively [11]. This differential suggests that the energetic cost of desolvating the backbone is overcome by enhanced stability upon formation of secondary structure in a bilayer. This principle underlies the requirement that membrane proteins must form secondary structure in a membrane [12].

Other general themes for membrane protein structure have emerged. The distribution of amino acids in transmembrane helices has evolved to foster favorable interactions with the water–lipid interface and the hydrophobic core [13]. There is an asymmetric distribution of residues on the N- and C-terminus of membrane proteins, with some polar residues, such as arginine and lysine, more abundant on the N-terminus on account of "snorkeling" effects [5]. The amphipathic residues tyrosine and tryptophan are localized at the bilayer interface and form an aromatic belt region that may serve as the protein anchor in the membrane [14,15]. As expected, aliphatic amino acids are more prevalent in the hydrophobic core of the lipid bilayer, resulting in membrane protein surfaces that are more hydrophobic than their interior [16,17].

Our understanding of membrane protein folding is inferior to our knowledge of membrane protein structure. For α-helical systems, a sequence of events has been described [8,12,18–20]: (i) interfacial partitioning, (ii) interfacial folding, (iii) insertion into the bilayer, and (iv) assembly of tertiary and quaternary structure in the bilayer. For β-barrel membrane proteins, a concerted mechanism of insertion and folding has been discussed [21]. It should be noted that these and other models for membrane protein folding are derived from a small set of proteins because of experimental difficulties. The challenge lies not only in identification of membrane proteins that undergo reversible folding, but also in successful application of a breadth of techniques to the membrane protein folding problem.

One system that has been utilized to elucidate folding mechanisms is the 325-residue outer membrane protein A (OmpA). OmpA is a major structural component of the *E. coli* outer membrane, and

☆ This article is part of a Special Issue entitled: Membrane protein structure and function.

* Corresponding author at: UC San Diego, 9500 Gilman Drive, MC 0314, La Jolla, CA 92093-0314, USA. Tel.: +1 858 534 8080.
E-mail address: judyk@ucsd.edu (J.E. Kim).

0005-2736/$ – see front matter © 2011 Elsevier B.V. All rights reserved.
doi:10.1016/j.bbamem.2011.08.029

also functions as a non-specific pore and phage receptor [22,23]. The N-terminus constitutes the transmembrane domain (171 residues) and the C-terminus constitutes the periplasmic region (154 residues). The transmembrane domain folds into a β-barrel pore that is comprised of eight antiparallel β-sheets; the structure of the periplasmic domain has not been resolved. OmpA serves as an ideal model system to study membrane protein folding because of the availability of high resolution NMR [24] and X-ray [25] structures, ease of purification [26], and ability to reversibly and spontaneously fold into lipid vesicles [27]. Additionally, there is significant prior work by our group and others on the photophysics, thermodynamics, and kinetics associated with the native tryptophan residues [15,28–30] that serve as chromophores in spectroscopic studies.

Utilization of techniques that report on global structural changes during a folding reaction enhances our comprehension of folding mechanisms. Förster resonance energy transfer (FRET) is a mechanism for energy transfer based on dipole–dipole interaction between donor and acceptor molecules that are separated by distance r. The efficiency for energy transfer scales as $1/r^6$, and this strong distance-dependence enables FRET to be a sensitive spectroscopic ruler for measuring separations between 10 and 100 Å [31]. Widespread availability of spectroscopic tools and the relative ease of site-specific attachment of extrinsic or intrinsic chromophores have facilitated a large number of FRET-based studies of proteins and oligonucleotides. For example, FRET has been used to measure intra- and intermolecular distances in large protein complexes, detect fluctuations in DNA, and probe the folding landscape of heme proteins [32–34]. Recent experiments have focused on single-molecule FRET measurements of biomolecular dynamics [35–38]. FRET has also been applied to a limited number of membrane-bound systems to determine structures of peptides in membranes [39,40], probe conformational changes in ion channels [41], and investigate helix–helix associations [42]. These and other examples of biological FRET exemplify the wealth of knowledge that may be gained from this technique, and motivate our present study to elucidate the complex mechanisms of membrane protein folding using this powerful tool.

2. Materials and methods

2.1. Expression and purification of OmpA mutants

The procedure for expression, isolation, and purification of OmpA mutants is described elsewhere [28]. The starting plasmid was one that encoded for a cysteine-free, all-phe mutant of OmpA in which the five native tryptophan residues at positions 7, 15, 57, 102, and 143 were substituted with phenylalanine residues. Additionally, the C-terminal periplasmic domain was cleaved by introduction of a stop codon at position 177. This truncated, trp-free mutant consists of only the transmembrane domain, and is referred to as W0Δ(177–325). For simplicity, we omit designation of the deleted residues and abbreviate the notation as W0Δ, where Δ indicates Δ(177–325). Three types of truncated OmpA systems were generated from this initial W0Δ mutant for the current study: OmpA with a single tryptophan residue as the donor, OmpA with a single cysteine residue on which the 1,5-IAEDANS (dns) acceptor moiety may be covalently linked, and OmpA with both tryptophan and cysteine residues (donor + acceptor). Four donor–acceptor pairs as well as appropriate control systems were generated: donor at position 15 with acceptor at position 7 (F15W/F7CdnsΔ); donor at position 57 with acceptor at position 7 (F57W/F7CdnsΔ); donor at position 143 with acceptor at position 7 (F143W/F7CdnsΔ); donor at position 143 with acceptor at position 57 (F143W/F57CdnsΔ); donor-only at position 15 (F15WΔ); donor-only at position 57 (F57WΔ); donor-only at position 143 (F143WΔ); acceptor-only at position 7 (F7CdnsΔ); and acceptor-only at position 57 (F57CdnsΔ). These mutants are summarized in Table 1, and distances between β-carbons from the X-ray structure are illustrated in Fig. 1.

2.2. Labeling

Purified OmpA (~70 μM in 4–5 mL) was initially mixed with tenfold excess reducing agent, tris(2-carboxyethyl)phosphine (TCEP) (stock concentration of 10 mM), and stirred under nitrogen for 1 h. Tenfold excess dns acceptor (1,5-IAEDANS is 5-((((2-iodoacetyl)amino)ethyl) amino)naphthalene-1-sulfonic acid, Molecular Probes) initially dissolved to 2–3 mM in dimethyl sulfoxide (DMSO) was added to the solution and allowed to react with the free cysteine residue at position 7 or 57 for approximately 5 h under nitrogen atmosphere. The reaction was quenched by addition of tenfold excess 2-mercaptoethanol (2-ME). Unreacted dns was separated from the protein by passing the sample down a desalting column (10-DG, Bio-Rad). The labeled OmpA sample was washed several times with fresh 20 mM phosphate (KP_i) buffer (pH 7.3) that contained 8 M urea, concentrated, and stored at −80 °C. Labeling yields were 66% (F143W/F57CdnsΔ), 100% (F57W/F7CdnsΔ), 100% (F15W/F7CdnsΔ), and 45% (F143W/F7CdnsΔ). These yields were determined from the UV–vis spectra and knowledge of the extinction coefficients: ε(337 nm, dns) = 5700 $cm^{-1}\,M^{-1}$; ε(280 nm, dns) = 4220 $cm^{-1}\,M^{-1}$; ε(280 nm, transmembrane OmpA with single tryptophan) = 26,020 $cm^{-1}\,M^{-1}$; and ε(280 nm, transmembrane OmpA with no tryptophan) = 20,500 $cm^{-1}\,M^{-1}$.

2.3. Preparation of vesicles

Small unilamellar vesicles (SUVs) were prepared following a published procedure [28]. Briefly, 20 mg of 1,2-dimyristoyl-sn-glycero-3-phosphocholine (DMPC, Avanti Polar Lipids) or 1,2-dipalmitoyl-*sn*-glycero-3-phosphocholine (DPPC, Avanti Polar Lipids) was dried under nitrogen gas. DMPC was utilized to probe the folding and insertion of OmpA while DPPC provided an opportunity to probe the adsorbed, but not inserted, state of OmpA [27,29]. The lipid was resuspended in 20 mM KP_i buffer to a final concentration of 5 mg/mL. The aqueous solution of lipid was placed in a warm water bath and sonicated with a probe ultrasonicator microtip for 1 h at 50% duty cycle. The SUV sample was then passed through a 0.22 μm filter, and equilibrated overnight at 37 °C prior to experiments.

2.4. Fluorescence and anisotropy measurements during folding reaction

Steady-state fluorescence measurements were performed with a Jobin Yvon-SPEX Fluorolo FL3-11 spectrofluorometer in a right-angle geometry using a 1 cm × 4 mm pathlength fused silica cuvette sealed with a rubber septum. The sample was excited along the 4 mm path, and emission was collected along the 1 cm path. The excitation wavelength for tryptophan was 290 nm, and that for the dns label was 330 nm. The excitation and emission bandpass were set to 4 nm for all unpolarized fluorescence spectra. The folding reaction was initiated by mixing a small volume of stock protein into an equilibrated SUV

Table 1
Summary of OmpA mutants. Residue positions of donor (D) and acceptor (A) as well as description of D and A locations are indicated. Residue at position 7 is located on the extra-vesicular side, and residues at positions 15, 57, and 143 are located on the intra-vesicular portion of the liposome.

Mutant	D	A	Description
F15W/F7CdnsΔ	15	7	D–A on same strand, across bilayer
F57W/F7CdnsΔ	57	7	D–A across bilayer
F143W/F7CdnsΔ	143	7	D–A across bilayer
F143W/F57CdnsΔ	143	57	D–A across pore
F15WΔ	15	–	Donor-only
F57WΔ	57	–	Donor-only
F143WΔ	143	–	Donor-only
F7CdnsΔ	–	7	Acceptor-only
F57CdnsΔ	–	57	Acceptor-only

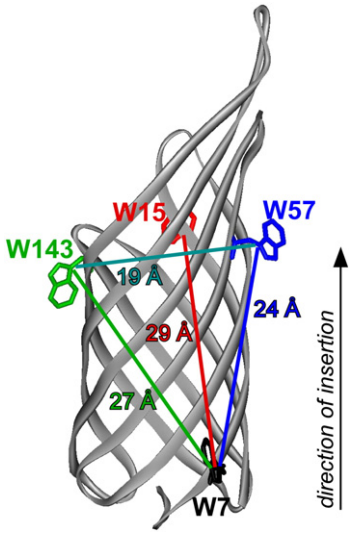

Fig. 1. Structure of OmpA transmembrane domain (PDB ID: 1QJP) highlighting native residues in locations of tryptophan donor (positions 15, 57, and 143) or cysteine-linked dns acceptor (positions 7 and 57). Distances between β-carbons are indicated. Residue W7 is located on the extra-vesicular portion of the liposome. Residues W7 and W15 are on the same strand. The unidirectional nature of insertion is shown.

solution with constant stirring. Fluorescence spectra were acquired at specified time points following mixing: 2, 5, 10, 15, 20, 25, 30, 40, 50, 60, 120, 180, and 240 min. The final solution in these folding experiments contained ~6 μM OmpA, 0.5 M urea, 1 mg/mL DMPC in 20 mM KPi buffer at pH 7.3. The solution was kept at 33 °C during folding experiments in order to maintain DMPC in the fluid phase ($T_m = 23$ °C) or DPPC in the gel phase ($T_m = 41$ °C). Spectra of SUV solutions that lacked protein were acquired at the beginning and end of each experiment.

Two additional experiments were performed to probe the contribution of aggregation and photobleaching to the observed signal. The extent of aggregation was measured under the same conditions as the folding experiments, with the exception that SUVs were excluded from the sample. Aggregation was monitored via a blue-shift in the emission maximum; for example, F143WΔ exhibited a fluorescence maximum of 337 nm after incubating for 3 h in 0.2 M urea solution. Photobleaching experiments were performed by injecting protein into a 20 mM KP_i/8 M urea solution, and monitoring the fluorescence spectra over a 240 minute window. These experiments confirmed that aggregation and photobleaching do not significantly contribute to the fluorescence spectra reported here.

Fluorescence anisotropy experiments were repeated twice under the same sample geometry conditions as the unpolarized fluorescence experiments. The polarized excitation wavelength was 290 nm, and polarized emission was obtained from 305 to 420 nm in 2 nm steps with excitation and emission bandpass set to 3 nm. Polarized spectra in the form of VV, VH, HV, and HH, where the first and second letters correspond to excitation and emission polarizations (V = vertical, H = horizontal), respectively, were acquired. Spectra of vesicle solutions that do not contain OmpA were also acquired and subtracted from corresponding OmpA spectra to remove contribution from scattering. The instrument response (G-factor) was determined using the model compound N-acetyl-L-tryptophanamide (NATA) and protein solutions; the G-factor was identical to within 5% when measured with these different samples.

3. Results

3.1. Folding yields for labeled protein

Donor–acceptor labeled OmpA was confirmed to fold and unfold via a gel-shift assay [28,43]. The labeled protein exhibited a folding yield of at least 70% after a 24-hour incubation period in lipid solution (Fig. S1). The yield of unfolding was ~90% after a 24-hour incubation period in 5 M urea solution. These yields are comparable to those observed for unlabeled transmembrane OmpA [28].

3.2. FRET calculations and data

Spectral overlap of the donor–acceptor (tryptophan–dns) pair was measured for folded and unfolded OmpA. Fig. 2 shows representative emission spectra of tryptophan in OmpA in the folded ($\lambda_{max} = 330$ nm) and unfolded ($\lambda_{max} = 350$ nm) states along with the absorption spectrum of model compound dns in aqueous solution. The absorption peak of dns that is covalently linked to folded or unfolded OmpA differs by less than 2 nm from the spectrum in aqueous solution (data not shown). The emission maximum of OmpA adsorbed on DPPC bilayers is between 339 and 347 nm, and depends on mutant (data not shown). Förster distances for the tryptophan–dns pair in OmpA can be calculated via the equation $R_0^6 = (8.79 \times 10^{23})(\kappa^2 n^{-4} \Phi_D J_{DA})$ where R_0 is the Förster distance (in Å), κ^2 is the orientation factor between the transition dipoles of the donor and acceptor (ranges from 0 to 4), n is the refractive index of the solvent, Φ_D is the quantum yield of the donor in the absence of acceptor, and J_{DA} is the overlap integral of the donor emission and acceptor absorption spectra [31,44,45]. For the unfolded state, we utilized the experimental absorption and emission spectra, and assumed values of 2/3 for κ^2, 0.13 for Φ_D, and 1.33 for n to calculate a Förster distance of 20.9 Å, which is consistent with prior published values of R_0 for the trp–dns pair [44,45]. The R_0 value for the folded state is 20.8 Å and was calculated using the appropriate overlap integral and the same values of κ^2, Φ_D, and n as the unfolded state. When a range of Φ_D values between 0.13 and 0.25 was utilized, the R_0 value varied 11.5% for the folded state. In contrast to minor changes in R_0 because of shifts in spectral profile and quantum yield, alterations in κ^2 can have a significant impact on the Förster distance (discussed below).

FRET efficiencies were calculated for the four donor–acceptor labeled mutants with the following equation [45]:

$$E = 1 - \frac{F_{DA} - F_D(1 - f_A)}{F_D f_A} = \left(1 - \frac{F_{DA}}{F_D}\right)\frac{1}{f_A} \quad (1)$$

where E is the FRET efficiency, F_{DA} and F_D are the fluorescence intensity of the donor (tryptophan) in the presence and absence of dns acceptor, respectively, and f_A is the labeling yield for the specific mutant. F_{DA} and F_D were determined for each mutant as a function of time after mixing. Representative fluorescence data for donor–acceptor labeled OmpA,

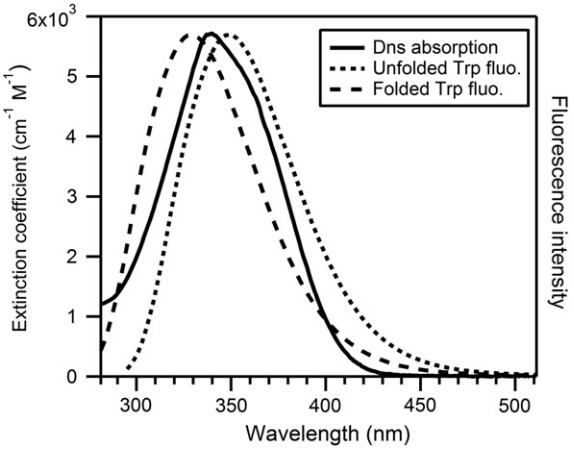

Fig. 2. Absorption spectrum of dns acceptor (solid, left axis). Normalized fluorescence spectra of tryptophan donor in unfolded (dotted) and folded (dashed) OmpA are also shown (right axis).

donor-only OmpA, and acceptor-only OmpA are shown in Figs. 3 and 4; additional data are included in supporting information (Fig. S2). FRET efficiencies are shown in Fig. 5. For all mutants except F15W/F7CdnsΔ, evolution of the FRET efficiencies is consistent with donor and acceptor moving toward each other as the protein folds and inserts into the bilayer. For these mutants, the FRET efficiencies evolve from as low as ~10% (unfolded in 8 M urea) to as high as 100% during the folding reaction. The fourth mutant in which donor and acceptor are on the same strand (F15W/F7CdnsΔ) displays the opposite trend in which donor and acceptor are moving apart, evidenced by the change in FRET efficiency from ~60% to ~0% during folding. FRET efficiencies for partially folded OmpA adsorbed on DPPC bilayers also indicated in Fig. 5. The estimated error for calculated FRET efficiencies is 20% for all mutants except F143W/F7CdnsΔ, and primarily reflects certainty in knowledge of labeling yields and protein concentrations. The error for the fourth mutant, F143W/F7CdnsΔ, is much larger (approximately 50%) because of the low labeling yield. It should be noted that the indicated FRET efficiencies have not taken into account the minor population of protein that does not fold. The percentage of unfolded protein is expected to be similar for all mutants at less than 30%, and this unfolded population should exhibit no spectral shifts throughout the observation window. Therefore, this systematic error would impact the absolute FRET efficiencies, but not the shapes, of the FRET curves during a folding reaction.

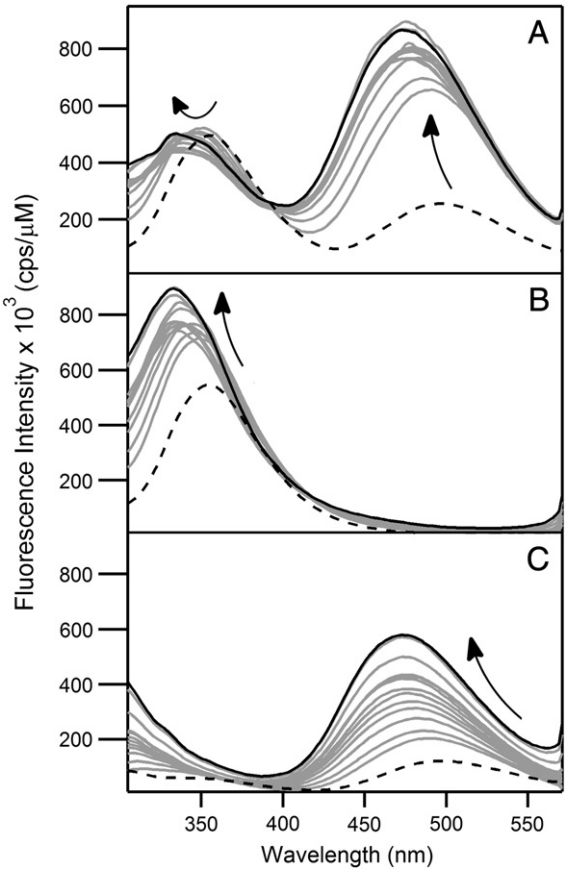

Fig. 3. Fluorescence spectra during folding (gray and black, solid) and for the unfolded state in 8 M urea (dashed). Spectrum of the folded state after 240 min is indicated as the solid, bold, black curve. Spectra are of (A) donor–acceptor labeled mutant F57W/F7CdnsΔ; (B) donor-only (F57WΔ) mutant; and (C) acceptor-only (F7CdnsΔ) mutant.

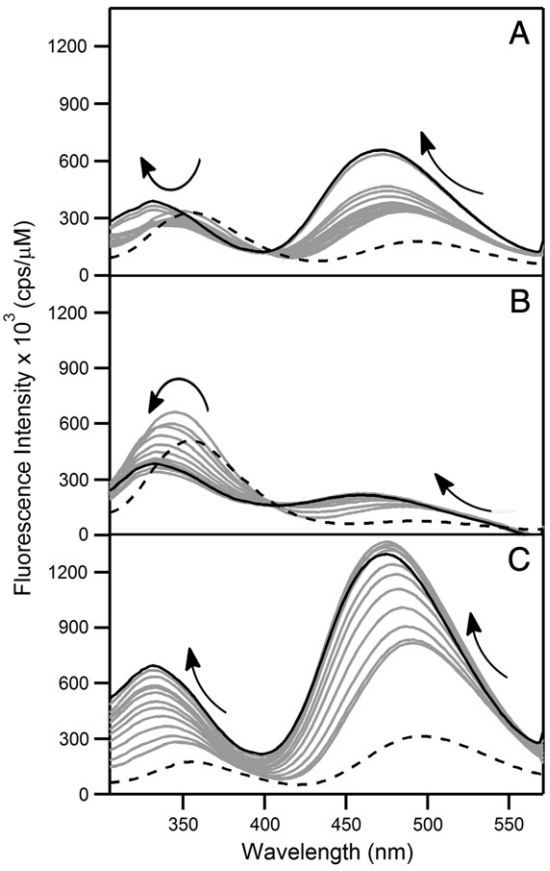

Fig. 4. Fluorescence spectra during folding (gray and black, solid) and for the unfolded state in 8 M urea (dashed). Spectrum of the folded state after 240 min is indicated as the solid, bold, black curve. Spectra are of donor–acceptor labeled mutants (A) F143W/F57CdnsΔ; (B) F143W/F7CdnsΔ; and (C) F15W/F7CdnsΔ.

3.3. Tryptophan fluorescence shift and anisotropy

The evolution of the tryptophan blue-shift as a function of folding time is shown in the supporting information (Fig. S3). The kinetic traces for six of the seven OmpA mutants studied here are similar and indicate that ~75% of the fluorescence shift is completed within 60 min. The donor–acceptor labeled mutant F143W/F57CdnsΔ exhibits a fluorescence shift that is about twofold slower. This result

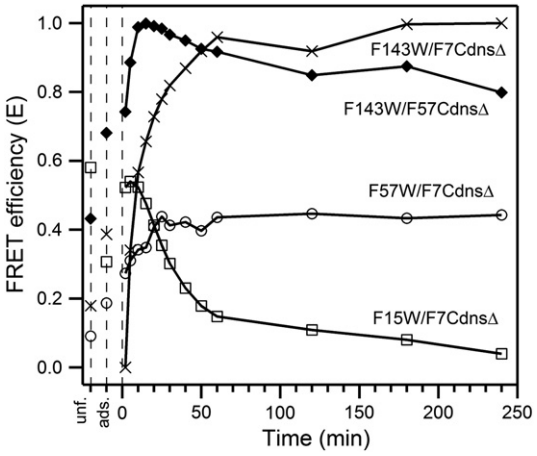

Fig. 5. FRET efficiency of unfolded state ("unf.") in 8 M urea, adsorbed species ("ads.") on DPPC, and during folding reaction into DMPC. Solid lines that connect the data points are included to help guide the eye. The estimated error for calculated FRET efficiencies is 20% for all mutants except F143W/F7CdnsΔ; the error for F143W/F7CdnsΔ is approximately 50%. See text for details.

indicates that traversal of the dns acceptor at position 57 through the bilayer may impede the folding kinetics (discussed below).

Steady-state anisotropy measurements were performed to investigate the rotational flexibility of the tryptophan donor during the folding event (Fig. 6). The enhanced anisotropy values of folded OmpA indicate loss of rotational flexibility in vesicles relative to unfolded OmpA in urea. In general, the anisotropy values are enhanced within minutes of initiating the folding reaction, and continue to increase on a timescale similar to those that characterize changes in FRET and tryptophan fluorescence. This finding supports a picture in which OmpA interacts closely with the membrane during folding, and this interaction gives rise to the measured anisotropy. The initial drop in anisotropy at t = 2 min for unfolded protein is likely an artifact that arises from injecting stock OmpA solution into the buffer solution; in this case, both solutions contain 8 M urea and are thus viscous. The implications of rotational restriction on FRET calculations are discussed below.

4. Discussion

4.1. Application of FRET to membrane protein folding

The application of FRET to membrane proteins is limited relative to analogous studies of soluble proteins because of challenges associated with the labeling and folding membrane proteins. Here we present FRET experiments on the 176-residue, transmembrane domain of OmpA. The selection of OmpA offers several advantages. First, β-barrel membrane proteins generally contain a greater fraction of polar residues than α-helical membrane proteins. A consequence of this property is that OmpA, unlike the α-helical protein bacteriorhodopsin, can be fully unfolded in denaturant, and refolded in the presence of lipid bilayer in a reversible and spontaneous manner [46]. Second, the availability of high-resolution structures [24,25] guides the design of appropriate FRET mutants. Finally, OmpA is a well-characterized system for membrane protein folding [15,21,28–30,47–50]. The observation that the transmembrane domain spontaneously inserts and folds into lipid bilayers in a unidirectional manner [27] is especially advantageous for these FRET measurements.

FRET mutants were selected for this initial study to probe the evolution of the following intraprotein distances: across the bilayer on different strands (F143W/F7CdnsΔ and F57W/F7CdnsΔ), across the bilayer on the same strand (F15W/F7CdnsΔ), and across the protein pore (F143W/F57CdnsΔ). The donor–acceptor pairs provide additional geometric constraints because three of the FRET pairs form the sides of a triangle, with donor and acceptor at the vertices. This combination of mutants enables study of the relative timescales for global structural changes, such as pore formation, bilayer traversal, and strand extension. The current experiments not only complement prior work that probed intermolecular protein–lipid distances with the use of brominated lipids [30,49], but may also enhance computational efforts in the expanding field of membrane protein folding.

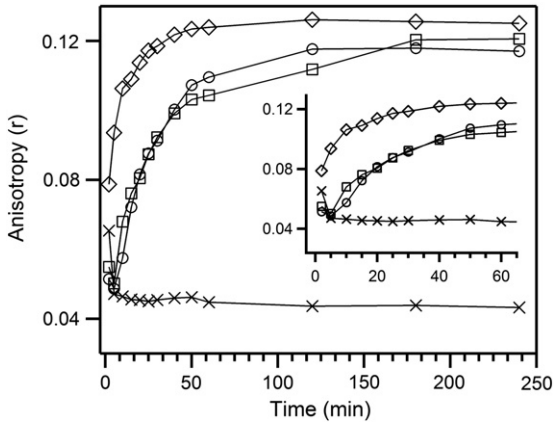

Fig. 6. Average values of tryptophan anisotropy in the range 330–360 nm for OmpA donor-only mutants during folding reaction into DMPC bilayers: (◇) F143WΔ; (□) F15WΔ; and (○) F57WΔ. OmpA that is injected into a solution of 8 M urea is also shown for (×) F143WΔ. An expanded view of the initial 65 min is shown as the inset. The upper limit for error in anisotropy is estimated as ±0.02.

Significant effort was devoted to characterizing the effect of labeling on the stability and kinetics of folding. The dns FRET acceptor has both hydrophobic (aromatic rings and hydrocarbon linker) and hydrophilic (sulfonate and amide groups) components and as a result, it is not straightforward to predict the effect of this extrinsic label on the folded state of OmpA. To our knowledge, there are no prior reports of *in vitro* FRET studies on membrane protein folding. Instead, a number of membrane proteins have been labeled with dyes on solvent-exposed residues to probe conformational changes and global interactions; nearly all of these examples utilized proteins in native membrane environments or solubilized in detergent [42,51–53]. As shown by SDS-PAGE analysis, dns-labeled OmpA inserts and folds into membranes with yields that are comparable to unlabeled OmpA. Additionally, the characteristic blue-shift of tryptophan fluorescence that accompanies folding [28,30] is preserved in the FRET mutants studied here. These measurements indicate that the presence of a covalently linked dns label at position 7 or 57 does not drastically alter the folded structure.

In contrast to these equilibrium measurements, the kinetics of insertion appears to be affected by the presence of a dns label at one of the positions. The single tryptophan residue at positions 15, 57 and 143 in the donor-only mutants of OmpA undergoes 75% of the fluorescence blue-shift within 60 min of folding. Attachment of a dns label at position 7 does not affect the kinetics. However, the presence of a dns label at position 57 impedes the kinetics such that the blue-shift occurs in ~100 rather than 60 min. One rational explanation for this perturbation is the unidirectional nature of insertion: residue 57 must traverse the bilayer whereas residue 7 is not required to cross the membrane. While it is plausible that the presence of the label at position 57 hinders the rate of insertion, we have not studied other OmpA mutants to confirm this hypothesis. Other experiments are currently underway.

4.2. Mechanisms of folding

An important goal of the present work is to elucidate mechanisms of folding. We acknowledge at the outset that the unfolded state in 8 M urea is not an adequate representation of the starting unfolded state for folding reactions. However, we pursued FRET measurements on OmpA in 8 M urea to investigate the protein in a presumably extended and unfolded conformation. The data in Fig. 5 indicate that as expected, the FRET efficiencies for donor and acceptor pairs that are distant in sequence are low in 8 M urea, typically less than ~45%. The exception is F15W/F7CdnsΔ, for which the donor and acceptor are eight residues apart on the same strand. For this mutant, the FRET efficiency in 8 M urea is high at ~60%, indicating that a dynamic loop is likely formed between donor and acceptor in this denaturant. The presence of a loop is consistent with theoretical predictions that the probability of loop formation is maximum for a loop length of ten [54].

Upon initiation of the folding event, the FRET results indicate that global changes occur on three different timescales. The most rapid change in FRET efficiency was observed for the mutant that reports on pore formation (F143W/F57CdnsΔ); this mutant exhibited a sharp increase in FRET efficiency that reached its maximum value of ~100% in 15 min, followed by a slow decay in FRET signal over the remaining collection period. Evolution of FRET signal occurred on an intermediate timescale for the two mutants that probe bilayer traversal, F143W/F7CdnsΔ and F57W/F7CdnsΔ. The FRET signal for both of these mutants began to level off in ~60 min, with no significant change following this initial rise. The slowest change in FRET efficiency

occurred for the mutant that probes strand extension across the bilayer, F15W/F7CdnsΔ. This mutant showed a large drop in FRET signal in the first 60 min, and continued to evolve until the last data point was measured at 240 min during the folding reaction.

The FRET data may be assembled to yield the following picture of OmpA insertion and folding into membranes (see Fig. 7). Because the insertion process is known to be directional, the pore is at least partially formed during insertion. Specifically, the inserting portion of the protein is likely to assemble as a compact pore as it inserts into the bilayer. This initial formation is consistent with the early FRET response of the F143W/F57CdnsΔ mutant. It appears that the presence of the dns label at position 57 (described above) does not impact the formation of the pore despite its apparent effect on insertion kinetics. Bilayer traversal occurs on a slower timescale, on the order of 60 min. Here, the term "bilayer traversal" is not intended to suggest that the bilayer is a static medium in which the protein inserts. Rather, the dynamic nature of the bilayer plays a critical role in the folding process and therefore, it is more appropriate to consider "lipid-assisted protein folding" in which there are simultaneous changes in both protein and bilayer structures during folding [29,55,56]. However, since the current studies are limited to intraprotein FRET, we attribute the formation of a membrane-spanning domain to bilayer traversal. Following this ~60-minute period of bilayer traversal, a long-time component that is attributed to strand extension and pore expansion persists over the 240-minute measurement window.

We also investigated the FRET signal for adsorbed intermediates that exhibit secondary structure, but does not insert into bilayers that are in the gel phase of DPPC [47]. For the three mutants in which donor and acceptor are distant in primary sequence, the adsorbed intermediates exhibited FRET efficiencies that are consistent with a compressed tertiary structure. This structure is more compact than the extended conformations in 8 M urea, but less compact than folded protein. The fourth mutant (F15W/F7CdnsΔ), in which the donor and acceptor are eight residues apart, shows the opposite trend where the adsorbed species is more extended than the unfolded state, but more compact than the folded species. These results suggest that while the β-sheet secondary structure of the adsorbed state resembles that of the folded state [27,57], the tertiary structures of the adsorbed and folded states are dissimilar.

Results from the present FRET experiments build upon prior studies of OmpA that utilized tryptophan fluorescence, circular dichroism, and SDS-PAGE analyses [21,30,57–59]. In these earlier reports, three membrane-associated intermediates were identified, and the kinetics of folding was found to depend on several factors, including pH, temperature, and membrane properties. The emerging picture for the folding mechanism includes initial formation of an adsorbed (collapsed) intermediate, followed by folding and insertion into the membrane in a concerted manner [21]. Our results support this concerted picture, and provide additional insight into changes in tertiary structure. One important conclusion from the FRET measurements is that the pore appears to form early during the folding reaction, prior to completion of bilayer traversal and secondary structure formation. This pore formation may be associated with adsorption. It should be noted that we do not yet know the full extent of pore formation because the FRET pair is located on the inserting portion of the protein. We are currently pursuing FRET measurements to monitor pore formation on the other end of the protein pore, near W7. Additional insight from the current studies is that the kinetics of bilayer traversal is coincident with the known blue-shift in fluorescence, and both occur on the order of ~60 min. This result suggests that the majority of the fluorescence blue-shift reported here and in prior reports can be attributed to formation of the membrane-spanning structure. Finally, the long-time component (~60–240 min) of folding that is observed as slow changes in the FRET signal and tryptophan fluorescence intensity (data not shown) may be attributed to equilibration of the protein in the bilayer. The current FRET results suggest that this equilibration may involve strand extension and pore expansion. This relaxation may also reflect slow changes in local solvation, such as expulsion of water from the protein/bilayer core. While this interpretation is consistent with prior reports, the current FRET data do not exclude the possibility of parallel folding pathways that exhibit different kinetics.

4.3. Interpretation of FRET distances

The conversion from FRET efficiency to intramolecular distance is, in principle, a straightforward task. However, for membrane proteins, we face several challenges. Here, we have shown that evolution of the absorption and emission profiles as well as the emission quantum yield during folding does not significantly alter the Förster distance for a given orientation factor; if orientational averaging of the donor and acceptor is assumed ($\kappa^2 = 2/3$), R_0 is calculated as 21 Å for the folded and unfolded states. However, it is possible that the use of 2/3 for κ^2 is not valid for folded OmpA, as has been discussed for dns-labeled bacteriorhodopsin [60]. Some deviation from the average value of 2/3 is supported by steady-state and time-resolved fluorescence anisotropy measurements that indicate that the donor is rotationally hindered when OmpA is inserted and folded in a bilayer [61].

The experimental difficulties of measuring the orientational factor have not precluded the wide use of FRET as a spectroscopic ruler. One reason for the quantitative success of FRET is that for systems that contain a heterogeneous population of conformations, the assumption of orientational averaging is valid [62]. For the majority of proteins in which donor and acceptor are covalently linked to solvent-exposed regions of the protein via flexible linkers, this assumption likely holds true. For OmpA and other membrane proteins, however, it is not known whether the folded protein exhibits preferential

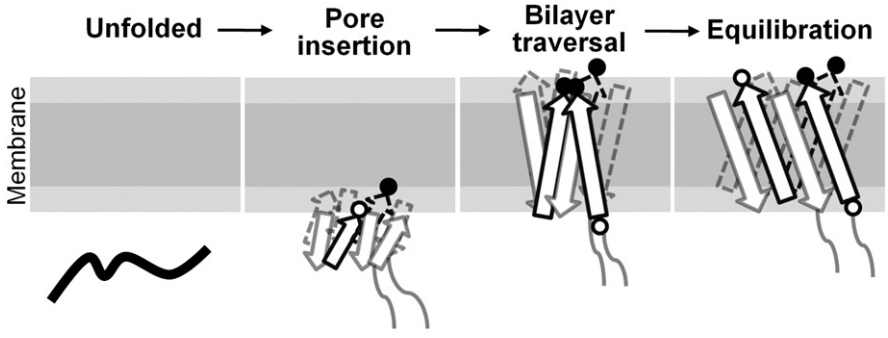

Fig. 7. Schematic of OmpA folding into a membrane. Hydrophobic core and interfacial space of lipid bilayer are indicated as dark and light gray shaded regions, respectively. OmpA that is initially unfolded in 8 M urea forms at least a partial pore that begins to insert into the bilayer within the first 15 min of initiating the folding reaction. The protein continues to insert and traverse the bilayer for approximately 60 min following initiation. A long-time equilibration period lasts up to at least 240 min, during which period OmpA undergoes strand extension and pore expansion. Timescales and structural changes are based on evolution of FRET signal of specific donor (closed circle) and acceptor (open circle) pairs on the protein. See main text for additional details.

orientations of donor and acceptor within the membrane. The structural restrictions that complicate the interpretation of FRET data for membrane proteins can be overcome by selection of appropriate donor–acceptor pairs. In the case of tryptophan and dns, both molecules exhibit more than one transition dipole moment associated with overlapping electronic transitions [63–65]. The presence of these near-degenerate transitions significantly limits the range of possible κ^2 values such that errors in distances are likely less than 10% [65]. Therefore, the combination of structural heterogeneity and optimized photophysical properties enables FRET to be a useful probe despite the challenges associated with the orientation factor.

In the case where a protein structure is available, comparison of the apparent FRET distances, r' (using $\kappa^2 = 2/3$), with those from the crystal/NMR structure may provide insight into the extent of conformational heterogeneity [31]. The use of $\kappa^2 = 2/3$ for a membrane protein is not unprecedented, and was justified in a previous study of helix–helix interactions of bacteriorhodopsin [42]. The evolution in distances between donor and acceptor for OmpA is summarized in the following form: r in 8 M urea → r' folded in membrane (with crystal structure distances from Fig. 1 in parentheses). The distance changes are 31 Å → 22 Å (24 Å) for donor and acceptor across the bilayer (F57W/F7Cdns∆), 27 Å → 13 Å (27 Å) for donor and acceptor across the bilayer (F143W/F7Cdns∆), 22 Å → 16 Å (19 Å) Å for donor and acceptor across the pore (F143W/F57Cdns∆), and 20 Å → 31 Å (29 Å) for donor and acceptor on the same strand across the bilayer (F15W/F7Cdns∆). Satisfactory agreement between FRET and crystal structure distances for folded protein is achieved for three mutants, suggesting that κ^2 may not significantly deviate from the value of 2/3. This finding is consistent with other reports that indicate variation in κ^2 do not result in significant error [44,66,67]. The fourth mutant, F143W/F7Cdns∆, exhibits a folded distance that is much smaller than expected given that the donor and acceptor must span the bilayer. This discrepancy likely arises because of the low labeling yield of 45% for this particular mutant, and this finding emphasizes the importance of high yields to obtain reliable results. Despite the overall agreement between crystallographic and FRET-based distances for the three mutants with high labeling yields, a more rigorous treatment of κ^2 would be necessary to confirm the absolute distances during folding [31,60,68,69]. Nonetheless, the qualitative trends reported here are likely to be valid.

5. Conclusion

The results presented here illustrate the application of FRET to the study of membrane protein folding. FRET experiments are advantageous because they provide insight on intraprotein distances during a folding event, and results from this technique complement existing knowledge about secondary structure and local environment that is gained from other tools. Relative timescales for global changes, such as protein pore formation, bilayer traversal, and strand extension, help elucidate the mechanisms of protein insertion and folding into a synthetic bilayer. Despite the relative success of these initial FRET experiments, it is clear that several challenges persist. Low labeling yields and lack of knowledge of the orientation factor hinder facile quantitative assessment of distances. Nonetheless, qualitative insight is gained and motivates ongoing FRET experiments on membrane protein folding.

Acknowledgements

G.K. was supported by Heme and Blood Proteins Training Grant T32-DK007233. I.L.P. received funding from a National Science Foundation Alliance for Graduate Education and the Professoriate Fellowship (HRD-0450366), and C.G. acknowledges support from the UCSD Chancellor's Undergraduate Research Scholarship. This work was supported by the National Science Foundation (CHE-0645720).

Appendix A. Supplementary data

Supplementary data to this article can be found online at doi:10.1016/j.bbamem.2011.08.029.

References

[1] J.N. Onuchic, Z. Luthey-Schulten, P.G. Wolynes, Theory of protein folding: the energy landscape perspective, Annu. Rev. Phys. Chem. 48 (1997) 545–600.
[2] K.A. Dill, H.S. Chan, From Levinthal to pathways to funnels, Nat. Struct. Biol. 4 (1997) 10–19.
[3] J.D. Bryngelson, P.G. Wolynes, Spin glasses and the statistical mechanics of protein folding, Proc. Natl. Acad. Sci. U.S.A. 84 (1987) 7524–7528.
[4] K.A. Dill, Dominant forces in protein folding, Biochemistry 29 (1990) 7133–7155.
[5] A.K. Chamberlain, Y. Lee, S. Kim, J.U. Bowie, Snorkeling preferences foster an amino acid composition bias in transmembrane helices, J. Mol. Biol. 339 (2004) 471–479.
[6] M.C. Wiener, S.H. White, Fluid bilayer structure determination by the combined use of X-ray and neutron diffraction. I. Fluid bilayer models and the limits of resolution, Biophys. J. 59 (1991) 162–173.
[7] E. Kaiser, F. Kezdy, Secondary structures of proteins and peptides in amphiphilic environments, Proc. Natl. Acad. Sci. U.S.A. 80 (1983) 1137–1143.
[8] W.C. Wimley, S.H. White, Experimentally determined hydrophobicity scale for proteins at membrane interfaces, Nat. Struct. Biol. 3 (1996) 842–848.
[9] J. Dilger, L. Fisher, D. Haydon, A critical comparison of electrical and optical methods for bilayer thickness determination, Chem. Phys. Lipids 30 (1982) 159–176.
[10] J.U. Bowie, Membrane protein folding: how important are hydrogen bonds? Curr. Opin. Struct. Biol. 21 (2011) 42–49.
[11] N. Ben-Tal, D. Sitkoff, I.A. Topol, A.S. Yang, S.K. Burt, B. Honig, Free energy of amide hydrogen bond formation in vacuum, in water, and in liquid alkane solution, J. Phys. Chem. B 101 (1997) 450–457.
[12] R.E. Jacobs, S.H. White, The nature of the hydrophobic binding of small peptides at the bilayer interface: implications for the insertion of transbilayer helices, Biochemistry 28 (1989) 3421–3437.
[13] M.B. Ulmschneider, M.S.P. Sansom, Amino acid distributions in integral membrane protein structures, Biochim. Biophys. Acta, Rev. Biomembr. 1512 (2001) 1–14.
[14] W.M. Yau, W.C. Wimley, K. Gawrisch, S.H. White, The preference of tryptophan for membrane interfaces, Biochemistry 37 (1998) 14713–14718.
[15] H. Hong, S. Park, R.H.F. Jiménez, D. Rinehart, L.K. Tamm, Role of aromatic side chains in the folding and thermodynamic stability of integral membrane proteins, J. Am. Chem. Soc. 129 (2007) 8320–8327.
[16] D. Rees, L. DeAntonio, D. Eisenberg, Hydrophobic organization of membrane proteins, Science 245 (1989) 510–513.
[17] F.A. Samatey, C. Xu, J.L. Popot, On the distribution of amino acid residues in transmembrane alpha-helix bundles, Proc. Natl. Acad. Sci. U.S.A. 92 (1995) 4577–4581.
[18] J.L. Popot, D.M. Engelman, Membrane protein folding and oligomerization: the two-stage model, Biochemistry 29 (1990) 4031–4037.
[19] J.L. Popot, D.M. Engelman, Helical membrane protein folding, stability, and evolution, Annu. Rev. Biochem. 69 (2000) 881–922.
[20] S.H. White, W.C. Wimley, Membrane protein folding and stability: physical principles, Annu. Rev. Biophys. Biomol. Struct. 28 (1999) 319–365.
[21] J.H. Kleinschmidt, Folding kinetics of the outer membrane proteins OmpA and FomA into phospholipid bilayers, Chem. Phys. Lipids 141 (2006) 30–47.
[22] Y. Wang, The function of OmpA in *Escherichia coli*, Biochem. Bioph. Res. Comm. 292 (2002) 396–401.
[23] E. Sugawara, H. Nikaido, Pore-forming activity of OmpA protein of *Escherichia coli*, J. Biol. Chem. 267 (1992) 2507–2511.
[24] A. Arora, F. Abildgaard, J.H. Bushweller, L.K. Tamm, Structure of outer membrane protein A transmembrane domain by NMR spectroscopy, Nat. Struct. Biol. 8 (2001) 334–338.
[25] A. Pautsch, G.E. Schulz, High-resolution structure of the OmpA membrane domain, J. Mol. Biol. 298 (2000) 273–282.
[26] M. Schweizer, I. Hindennach, W. Garten, W. Henning, Major proteins of the *Escherichia coli* outer cell envelope membrane. Interaction of protein II with lipopolysaccharide, Eur. J. Biochem. 82 (1978) 211–217.
[27] T. Surrey, F. Jahnig, Refolding and oriented insertion of a membrane protein into a lipid bilayer, Proc. Natl. Acad. Sci. U.S.A. 89 (1992) 7457–7461.
[28] K.M. Sanchez, J.E. Gable, D.E. Schlamadinger, J.E. Kim, Effects of tryptophan microenvironment, soluble domain, and vesicle size on the thermodynamics of membrane protein folding: lessons from the transmembrane protein OmpA, Biochemistry 47 (2008) 12844–12852.
[29] K.M. Sanchez, G.P. Kang, B.J. Wu, J.E. Kim, Tryptophan-lipid interactions in membrane protein folding probed by ultraviolet resonance Raman and fluorescence spectroscopy, Biophys. J. 100 (2011) 2121–2130.
[30] J.H. Kleinschmidt, T. den Blaauwen, A.J.M. Driessen, L.K. Tamm, Outer membrane protein A of *Escherichia coli* inserts and folds into lipid bilayers by a concerted mechanism, Biochemistry 38 (1999) 5006–5016.
[31] L. Stryer, Fluorescence energy transfer as a spectroscopic ruler, Annu. Rev. Biochem. 47 (1978) 819–846.
[32] M.E. Dockter, A. Steinemann, G. Schatz, Mapping of yeast cytochrome c oxidase by fluorescence resonance energy transfer — distances between subunit-II, heme-a, and cytochrome c bound to subunit-III, J. Biol. Chem. 253 (1978) 311–317.
[33] G. Bonnet, O. Krichevsky, A. Libchaber, Kinetics of conformational fluctuations in DNA hairpin-loops, Proc. Natl. Acad. Sci. U.S.A. 95 (1998) 8602–8606.

[34] J.G. Lyubovitsky, H.B. Gray, J.R. Winkler, Mapping the cytochrome c folding landscape, J. Am. Chem. Soc. 124 (2002) 5481–5485.
[35] X.W. Zhuang, H. Kim, M.J.B. Pereira, H.P. Babcock, N.G. Walter, S. Chu, Correlating structural dynamics and function in single ribozyme molecules, Science 296 (2002) 1473–1476.
[36] B. Schuler, E.A. Lipman, W.A. Eaton, Probing the free energy surface for protein folding with single-molecule fluorescence spectroscopy, Nature 419 (2002) 743–747.
[37] B. Schuler, W.A. Eaton, Protein folding studied by single-molecule FRET, Curr. Opin. Struct. Biol. 18 (2008) 16–26.
[38] R. Zhao, D. Rueda, RNA folding dynamics by single-molecule fluorescence resonance energy transfer, Methods 49 (2009) 112–117.
[39] W. Veatch, L. Stryer, The dimeric nature of gramicidin — a transmembrane channel — conductance and fluorescence energy transfer studies of hybrid channels, J. Mol. Biol. 113 (1977) 89–102.
[40] J.R. Lakowicz, I. Gryczynski, G. Laczko, W. Wiczk, M.L. Johnson, Distribution of distances between the tryptophan and the N-terminal residue of melittin in its complex with calmodulin, troponin C, and phospholipids, Prot. Sci. 3 (1994) 628–637.
[41] A. Cha, G.E. Snyder, P.R. Selvin, F. Bezanilla, Atomic scale movement of the voltage-sensing region in a potassium channel measured via spectroscopy, Nature 402 (1999) 809–813.
[42] S.J. Nannepaga, R. Gawalapu, D. Velaszuez, R. Renthal, Estimation of helix–helix association free energy from partial unfolding of bacterioopsin, Biochemistry 43 (2004) 550–559.
[43] L.K. Tamm, A. Arora, D. Rinehart, G. Szabo, Refolded outer membrane protein A of *Escherichia coli* forms ion channels with two conductance states in planar lipid bilayers, J. Biol. Chem. 275 (2000) 1594–1600.
[44] P.G. Wu, L. Brand, Resonance energy transfer: methods and applications, Anal. Biochem. 218 (1994) 1–13.
[45] J.R. Lakowicz, Principles of Fluorescence Spectroscopy, Springer, New York, 2006.
[46] P.J. Booth, R.H. Templer, W. Meijberg, S.J. Allen, A.R. Curran, M. Lorch, In vitro studies of membrane protein folding, Crit. Rev. Biochem. Mol. Biol. 36 (2001) 501–603.
[47] K. Dornmair, H. Kiefer, F. Jahnig, Refolding of an integral membrane protein — OmpA of *Escherichia coli*, J. Biol. Chem. 265 (1990) 18907–18911.
[48] H. Hong, L.K. Tamm, Elastic coupling of integral membrane protein stability to lipid bilayer forces, Proc. Natl. Acad. Sci. U.S.A. 101 (2004) 4065.
[49] J.H. Kleinschmidt, L.K. Tamm, Time-resolved distance determination by tryptophan fluorescence quenching: probing intermediates in membrane protein folding, Biochemistry 38 (1999) 4996–5005.
[50] M. Ramakrishnan, J. Qu, C.L. Pocanschi, J.H. Kleinschmidt, D. Marsh, Orientation of beta-barrel proteins OmpA and FhuA in lipid membranes. Chain length dependence from infrared dichroism, Biochemistry 44 (2005) 3515–3523.
[51] G. Harris, R. Renthal, J. Tuley, N. Robinson, Dansylation of bacteriorhodopsin near the retinal attachment site, Biochem. Biophys. Res. Comm. 91 (1979) 926–931.
[52] Y. Taniguchi, T. Ikehara, N. Kamo, Y. Watanabe, H. Yamasaki, Y. Toyoshima, Application of fluorescence resonance energy transfer (FRET) to investigation of light-induced conformational changes of the phoborhodopsin/transducer complex, Photochem. Photobiol. 83 (2007) 311–316.
[53] D.S. Majumdar, I. Smirnova, V. Kasho, E. Nir, X. Kong, S. Weiss, H.R. Kaback, Single-molecule FRET reveals sugar-induced conformational dynamics in LacY, Proc. Natl. Acad. Sci. U.S.A. 104 (2007) 12640–12645.
[54] C.J. Camacho, D. Thirumalai, Theoretical predictions of folding pathways using the proximity rule, with applications to bovine pancreatic trypsin inhibitor, Proc. Natl. Acad. Sci. U.S.A. 92 (1995) 1277–1281.
[55] W. Dowhan, M. Bogdanov, Lipid-assisted protein folding, J. Biol. Chem. 274 (1999) 36827–36830.
[56] W. Dowhan, M. Bogdanov, Lipid-dependent membrane protein topogenesis, Annu. Rev. Biochem. 78 (2009) 515–540.
[57] N.A. Rodionova, S.A. Tatulian, T. Surrey, F. Jaehnig, L.K. Tamm, Characterization of two membrane-bound forms of OmpA, Biochemistry 34 (1995) 1921–1929.
[58] J.H. Kleinschmidt, L.K. Tamm, Folding intermediates of a beta-barrel membrane protein. Kinetic evidence for a multi-step membrane insertion mechanism, Biochemistry 35 (1996) 12993–13000.
[59] J.H. Kleinschmidt, L.K. Tamm, Secondary and tertiary structure formation of the beta-barrel membrane protein OmpA is synchronized and depends on membrane thickness, J. Mol. Biol. 324 (2002) 319–330.
[60] R. Renthal, M. Cothran, N. Dawson, G.J. Harris, Fluorescent labeling of bacteriorhodopsin: implications for helix connections, Biochem. Biophys. Acta 897 (1987) 384–394.
[61] J.E. Kim, G. Arjara, J.H. Richards, H.B. Gray, J.R. Winkler, Probing folded and unfolded states of outer membrane protein A with steady-state and time-resolved tryptophan fluorescence, J. Phys. Chem. B 110 (2006) 17656–17662.
[62] A. Englert, M. Leclerc, Intramolecular energy transfer in molecules with a large number of conformations, Proc. Natl. Acad. Sci. U.S.A. 75 (1978) 1050–1051.
[63] J. Schlessi, Iz Steinber, I. Pecht, Antibody-hapten interactions — circular and linear polarization of fluorescence of dansyl bound to anti-dansyl antibodies, J. Mol. Biol. 87 (1974) 725–740.
[64] P.R. Callis, L-1(a) and L-1(b) transitions of tryptophan: applications of theory and experimental observations to fluorescence of proteins, Methods Enzymol. 278 (1997) 113–150.
[65] E. Haas, E. Katchalskikatzir, I.Z. Steinberg, Effect of orientation of donor and acceptor on probability of energy transfer involving electronic transitions of mixed polarization, Biochemistry 17 (1978) 5064–5070.
[66] C.G. dos Remedios, P.D.J. Moens, Fluorescence resonance energy transfer spectroscopy is a reliable ruler for measuring structural changes in proteins — dispelling the problem of the unknown orientation factor, J. Struct. Biol. 115 (1995) 175–185.
[67] J.R. Lakowicz, I. Gryczynski, W. Wiczk, G. Laczko, F.C. Prendergast, M.L. Johnson, Conformational distributions of melittin in water–methanol mixtures from frequency-domain measurements of nonradiative energy transfer, Biophys. Chem. 36 (1990) 99–115.
[68] M. Hoefling, N. Lima, D. Haenni, C.A.M. Seidel, B. Schuler, H. Grubmuller, Structural heterogeneity and quantitative FRET efficiency distributions of polyprolines through a hybrid atomistic simulation and Monte Carlo approach, PLoS One 6 (2011).
[69] B. Corry, D. Jayatilaka, B. Martinac, P. Rigby, Determination of the orientational distribution and orientation factor for transfer between membrane-bound fluorophores using a confocal microscope, Biophys. J. 91 (2006) 1032–1045.